arXiv:1510.02721v1 [math-ph] 9 Oct 2015

# Currents in the dilute $O(n = 1)$ loop model

G.Z. Fehér, B. Nienhuis

October 12, 2015

**Abstract**

In the framework of an inhomogeneous solvable lattice model, we derive exact expressions to boundary-to-boundary current on a lattice of finite width. The model we use is the dilute $O(n = 1)$ loop model, and our expression are derived based on solutions of the $q$-Kniznik-Zamolodchikov equations, and recursion relations.

## Contents

**1 Introduction** **2**

**2 The square lattice dilute loop model on a strip** **3**
2.1 Baxterization, inhomogeneous weights . . . . . 5
2.2 Vector space of link patterns, dilute Temperley-Lieb algebra . . . . . 8
2.3 Double row transfer matrix . . . . . 15

**3 Definition of current, main results** **17**
3.1 Boundary to boundary current . . . . . 17
3.2 Main result . . . . . 18

**4 Recursion relations** **19**
4.1 Fusion equation . . . . . 19
4.2 Boundary recursion relations . . . . . 21

**5 Symmetries** **23**
5.1 Symmetries of $Y_L$ . . . . . 23
5.2 Symmetries of $X_L$ . . . . . 26

**6 Proof of the main result** **26**
6.1 Proof for the $Y$ current . . . . . 26
6.2 Proof for the $X$ current . . . . . 28

**7 Acknowledgment** **29**

**APPENDIX** **29**

**A Normalization of the transfer-matrix** **29**

**B Construction of the open boundary $K$-matrix from the closed boundary $K$-matrix via insertion of a line** **31**

# 1 Introduction

In the last decades, a growing interest surround integrable loop models, which is fueled by connections to very distinct fields of combinatorics, correlation functions and discrete holomorphicity.
Loop models were originally introduced as high temperature expansions for spin model, or $n$-vector models. From the symmetry group in that language, they are now known as O($n$) loop models. Later an integrable version of the model was identified in [1, 2]. In [3] a set of finite difference equation, the –loosely called – quantum Kniznik-Zamolodchikov equations were introduced in order to find the partition sum and the groundstate elements of the dense $O(1)$ model with periodic boundary conditions. This approach was a fruitful ground for further research. It was used to extend the calculations to the groundstate of dense $O(1)$ loop model on a strip with open boundary conditions [4, 5] . Later, this approach was used to compute quantities not directly related to the groundstate of the transfer-matrix, e.g. left passage probability in percolations [6], current [7], correlation functions [8] (on finite temperature [9]). Observables has been computed in the dense $O(n = 1)$ model on a cylinder, for the homogeneous case [10, 11]. There was an attempt to prove the Razumov-Stroganov conjecture [12–14] (see also [15]) by this method [3, 16], which was finally proven by purely combinatorial method [17].
The motivation for this work is coming from several direction. The integrability of finite size lattice models provide a good ground to compute complicated quantities (e.g. correlations) exactly. In the scaling limit –when the lattice spacing disappear– many two dimensional lattice models believed to be conformal field theories. In this paper, we deal with a discretely holomorphic, parafermionic observable, the spin-1 boundary to boundary current (for further connection between integrability and discrete holomorphicity, look up e.g. [18, 19]). The premise of dealing with such observables is, that in the scaling limit of the lattice model, these observables turn into the holomorphic observables of the CFT. The model, we use for compute the quantities, is the dilute $O(n = 1)$ loop model.

We will study the statistical ensemble of non-intersecting paths on a strip of finite width and infinite height, in the framework of dilute loop model, which we are defining in Section 2. The paths may form closed loops, or terminate on the boundary. We assume, the paths connecting the two boundaries carry equal unit of current from the

left boundary to the right boundary. The closed loops, and paths connected only to one of the boundaries do not carry any current. In this paper, we are computing the mean current density induced by the statistics of the paths. Introduce the observable $F^{(x_1,x_2)}$, which is the mean current between points $x_1$ and $x_2$, oriented with $x_1$ to the left of the direction of the current:

$$F^{(x_1,x_2)} = \sum_{C\in\Gamma} P(C) N_C^{(x_1,x_2)} \mathrm{sign}_C^{(x_1,x_2)}. \tag{1}$$

Here $\Gamma$ is the set of all configurations, $N_C^{(x_1,x_2)}$ is the number of paths passing in between points $x_1$ and $x_2$ and running form the left to the right boundary, $P(C)$ is the ensemble probability of configuration $C$ and $\mathrm{sign}_C^{(x_1,x_2)}$ is $+1$ if $x_1$ lies in the region above the paths, and $-1$ if it lies below. The observable $F$ is antisymmetric, $F^{(x_1,x_2)} = -F^{(x_2,x_1)}$, and additive, $F^{(x_1,x_3)} = F^{(x_1,x_2)} + F^{(x_2,x_3)}$.

Up to a phase factor, $F$ is the $s = 1$ special case of the more general, arbitrary $s$ spin case:

$$\tilde{F}^{s,(x_1,x_2)} = \sum_{C\in\Gamma} P(C) N_C^{(x_1,x_2)} e^{is\phi(C)}, \tag{2}$$

where $\phi(C)$ is the winding angle from the starting direction until the crossing of the path with the $x_1$, $x_2$ line.

The dilute $O(n)$ model is related to the site percolation on a triangular lattice and the Izergin-Korepin type 19-vertex model [20, 21].

This work is a direct continuation of [22,23], where the groundstate elements and partition sum has been computed. This result is also an extension of [7], where the same current was computed for the dense $O(1)$ loop model.

The structure of the paper is as follows. In Section 2, we define the model, in Section 3, we present our main result, in Section 4, 5, we build up the necessary tools for our statements, and in Section 6, –under a technical assumption– we prove the main result. Further calculations are in the Appendix.

# 2 The square lattice dilute loop model on a strip

Consider a square lattice of width $L$ and infinite height. Each square of the lattice is decorated randomly by one of the nine plaquettes:

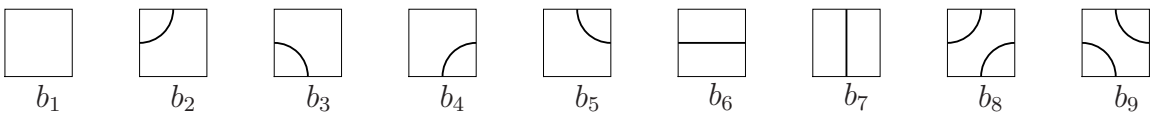

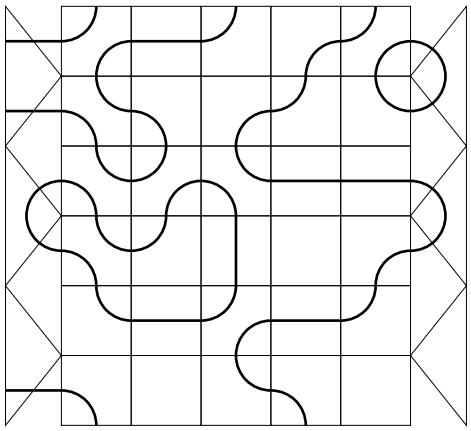

Figure 1: A typical configuration at $L = 5$

The decoration is subject to the restriction, that each line built up by the decoration of the plaquettes has to be continuous, so either end on the boundaries, either form a closed loop. Because certain configurations are not allowed, we can not associate *independent probabilities* with the plaquettes, we can only associate *statistical weights* with them. To describe the interaction with the left and right boundary, we introduce different kind of plaquettes, respectively:

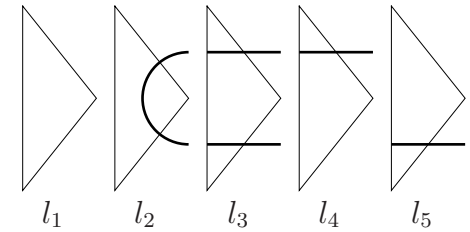


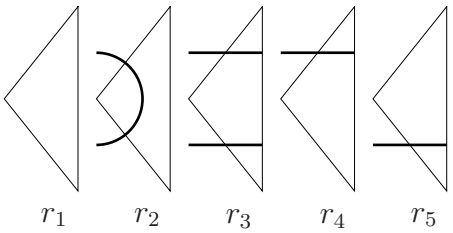


A typical configuration can be seen in Fig. 1. To assign probabilities with arbitrary finite or infinite configuration, we use the next definition: Each closed loop in the bulk carries the weight $n$, and each loop attached to the boundaries also carries the weight $n$. Also each plaquette carries a weight, given by the label in the pictures above. The

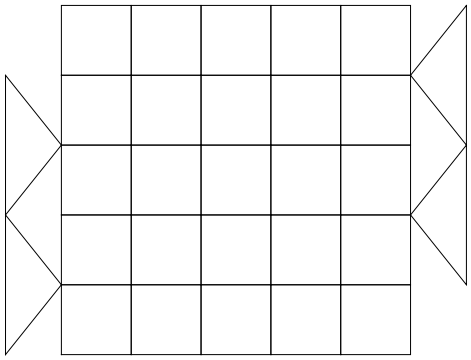

Figure 2: Zigzag B.C.

statistical weight of a configuration $C$ is given by the product of the weights of the constituent plaquettes and the weight of the loops:

$$P(C) = \left( \prod_{i=1}^{9} b_i^{\#\text{ of } b_i \text{ plaquettes}} \right) \left( \prod_{i=1}^{5} l_i^{\#\text{ of } l_i \text{ plaquettes}} \right) \left( \prod_{i=1}^{5} r_i^{\#\text{ of } r_i \text{ plaquettes}} \right) n^{\#\text{ of loops}} \quad (3)$$

We will deal only with the case $n = 1$, i.e. we can ignore the number of loops.

By this, we have defined the *homogeneous dilute O(n=1) loop model* [1, 2], with open boundary conditions.

There are some other subtleties, to define the model differently, we can distinguish the lines connecting the two boundaries from the ones connected to only one [19], we can introduce 'zigzag' boundary conditions, as in Fig. 2, we can introduce other boundary conditions by restricting the set of boundary plaquettes, we can introduce mixed boundary conditions by making this in a non-symmetric way, we can assign different $n$ and $n_1$ weights to loops in bulk and loops connected to the boundaries. Concerning the loop weights, we always choose $n = 1$, and an arbitrary but uniform weight for the paths terminating on the boundary. In practice this weight is incorporated in the local boundary weights. The different geometries of the underlying lattice do not change the results in an essential way. The lattice could also be drawn diagonally with respect to the boundaries.

## 2.1 Baxterization, inhomogeneous weights

In this section we define the *inhomogeneous* version of our model. To make our model accessible for the toolbox of integrability, we need to introduce inhomogeneous weights

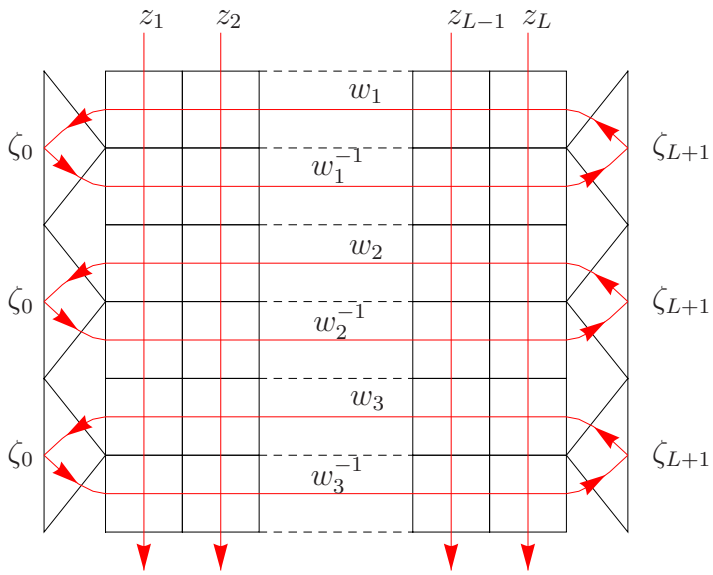


Figure 3: Rapidities

both for the bulk and boundary plaquettes, which satisify the Yang-Baxter [24] and the reflection equations [25]. To do so, we introduce *rapidities* flowing through the sites, according to Fig. 3.

By the Baxterization, we make the statistical weight of a plaquette be the function of the two rapidities crossing it. To make it explicit, we introduce the *R-matrix*:

$R(z,w) =$ 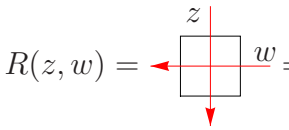 $= W_1(z,w)\Big($ $+$ $+$ $\Big) +$

$+ W_t(z,w)\Big($ $+$ $+$ $+$ $\Big) + W_2(z,w)$ $+ W_m(z,w)$ , (4)

with the next weights:

$$W_1(z,w) = -1 + \left(\frac{w}{z}\right)^2 \tag{5}$$

$$W_t(z,w) = \left(q + q^2\right)\frac{w}{z} \tag{6}$$

$$W_2(z,w) = q + q^2\left(\frac{w}{z}\right)^2 \tag{7}$$

$$W_m(z,w) = -q - q^2\left(\frac{w}{z}\right)^2. \tag{8}$$

Here $q = e^{i\pi/3}$. The $R$-matrix can be regarded in two different way: It can be regarded as the statistical weight of the plaquette, or as an operator. We need to introduce some more object to understand the $R$-matrix as an operator, so, we postpone this for later. The $R$-matrix is normalized by

$$W_R(z,w) = -1 - \frac{w}{z} + 2q\frac{w}{z} + \frac{w^2}{z^2} \tag{9}$$

which means that the $R$-matrix as a stochastical matrix, normalized to $W_R(z,w)$, so $R(z,w)/W_R(z,w)$ gives probabilities.

By the same way of thinking, we can introduce the left and right $K$-matrices, which describes the interaction with the boundaries:

$K_l(z,z_B) = z_B$ 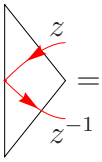 $= K^l_{id}(z,z_B)$ 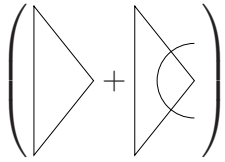 + (10)

$K^l_m(z,z_B)$ 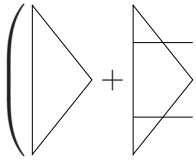 $+ K^l_1(z,z_B)$ 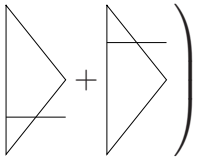 (11)

$K_r(z,z_B) =$ 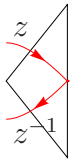 $z_B = K^r_{id}(z,z_B)$ 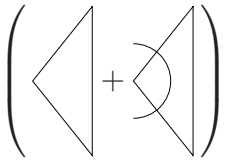 + (12)

$K^r_m(z,z_B)$ 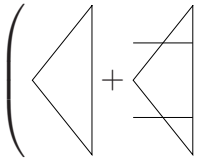 $+ K^r_1(z,z_B)$ 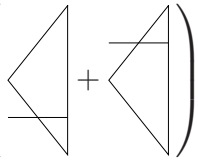 , (13)

with the next weights:

$$K^l_{id}(z,z_B) = k^2\left(z^{-1}\right)x^2\left(z_B\right) - 1 \tag{14}$$
$$K^l_m(z,z_B) = x^2(z_B)k\left(z^{-1}\right)\left(k(z) - k\left(z^{-1}\right)\right) \tag{15}$$
$$K^l_1(z,z_B) = x(z_B)\left(k(z) - k\left(z^{-1}\right)\right) \tag{16}$$

$$K^r_{id}(z,z_B) = 1 - k^2\left(z^{-1}\right)x^2\left(z_B\right) \tag{17}$$
$$K^r_m(z,z_B) = x^2\left(z_B\right)k(z)\left(k\left(z\right) - k\left(z^{-1}\right)\right) \tag{18}$$
$$K^r_1(z,z_B) = x(z_B)\left(k(z) - k\left(z^{-1}\right)\right) \tag{19}$$

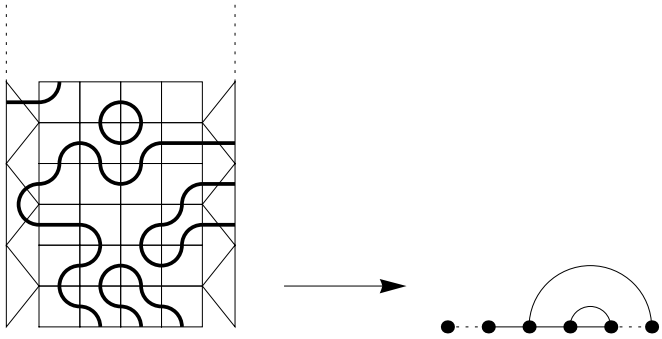

Figure 4: The mapping from loop configurations to link patterns. The two outermost points –connected with a dotted line to the others– represents the two boundaries. Here the image of the mapping is $|.(()\rangle$ .

Here, $z_B$ is a free parameter, which we will call *boundary rapidity*. The left and right $K$-matrix is normalized by

$$W_{K_l}(z,\zeta) = (k(z)x(\zeta)-1)\left(1+k\left(z^{-1}\right)x(\zeta)\right), \tag{20}$$

$$\tag{21}$$

$$W_{K_r}(z,\zeta) = \left(1-k\left(z^{-1}\right)x(\zeta)\right)(1+k(z)\,x(\zeta)), \tag{22}$$

respectively, and we use

$$k(z) = qz - z^{-1} \tag{23}$$

$$x(z) = q\frac{z}{z^2-1} \tag{24}$$

auxiliary functions.

By this definition, the weight of a given configuration is a function of the contributing rapidities.

## 2.2 Vector space of link patterns, dilute Temperley-Lieb algebra

To understand the $R$ and $K$-matrices as operators, and to precisely describe the Yang-Baxter and reflection equations, we need to introduce the dilute Temperley-Lieb-algebra and the vector space of link patterns (For a brief overview, see [26]).

We take the inhomogeneous dilute $O(n=1)$ loop model on an half-infinite strip, and we are interested in the connectivity configurations on the bottom edge.

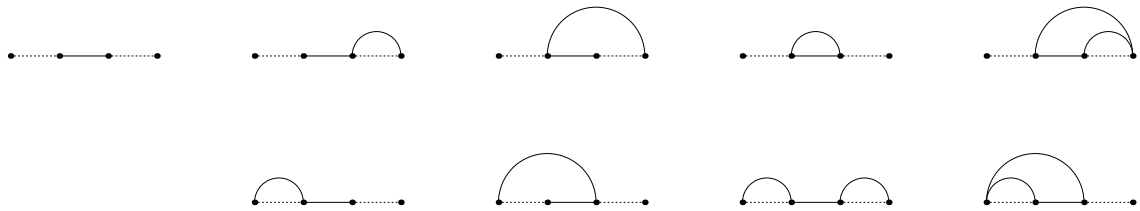

Figure 5: The basis elements of $dLP_{L=2}$. The top row: $|..\rangle$ (empty element), $|.(\rangle$, $|(.\rangle$, $|()\rangle$, $|((\rangle$. The bottom row: $|).\rangle$, $|.)\rangle$, $|)(\rangle$, $|))\rangle$.

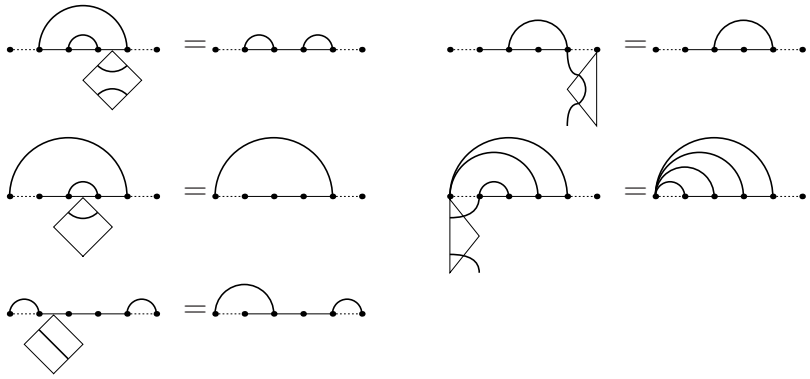

Figure 6: Some examples of $R$, and $K$-matrix elements acting on Temperley-Lieb states

Introduce $dLP_L$, the vector space of *dilute link patterns* of size $L$ the vector space of the connectivities, which is spanned by the possible connectivities. Every site can be either occupied or empty. If a site is occupied, it can be connected to an other site, or to one of the boundaries. Because of the non-crossing nature of the underlying model, the sites are connected without crossings. An example of this mapping is in Fig. 4. $dLP_L$ is in bijection with $L$ long strings of the characters (, . and ), consequently dim $dLP_L = 3^L$. As an example, the basis elements of $dLP_{L=2}$ are in Fig. 5.

The $R$-matrix and $K$-matrix act on the link pattern vector space as an operator. The image of a specific plaquette on a link pattern is the link pattern which is visible after attaching the given plaquette to the bottom. There are some examples in Fig. 6. The $R$-matrix is an element of the dilute Temperley-Lieb algebra. The $R$-matrix and $K$-matrix act as stochastic operators over $dLP_L$. $R$-matrix acts on two consecutive sites, where we need to specify that $R$ acts on sites $i$ and $i+1$, we will use the subscription: $R_{i,i+1}$. To compute the correct weights, $R$ and $K$-matrices should be considered as they always map from the two sites, where rapidities enter to the two, where they exit, and

their orientation is taken into account respecting this rule. Relations involving $R$ and $K$-matrices can be represented by drawings. The directed red lines always represent rapidity flows. A crossing of two rapidity flow is an $R$-matrix, its weight is computed respecting the direction of lines. We introduce lines for the boundary rapidities too, it is helpful to treat rapidities and boundary rapidities in a more uniform way. By this, we give new pictorial representation for the $K$-matrices:

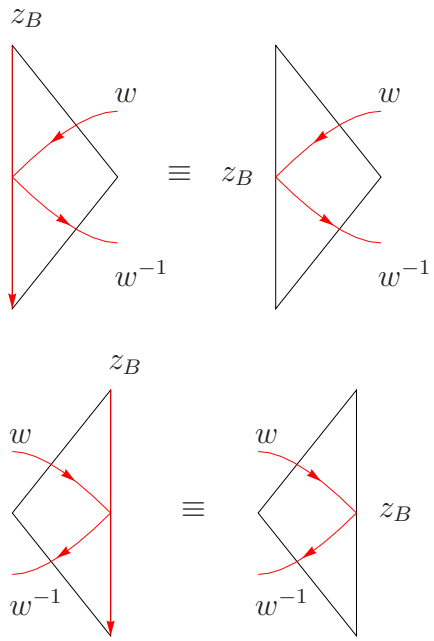


A reflection of a rapidity on a boundary is represented by a $K$-matrix. The order of the operators is prescribed by the direction of rapidities. The tiles are only drawn on some of the pictures.

With the previously mentioned definition, the $R$-matrix satisfies the next equations (In the figures, for legibility, we omit prefactors):

- the inversion/unitary relation:

$$R(z_2, z_1)R(z_1, z_2) = W_R(z_2, z_1)W_R(z_1, z_2) \cdot \mathrm{id} \tag{25}$$

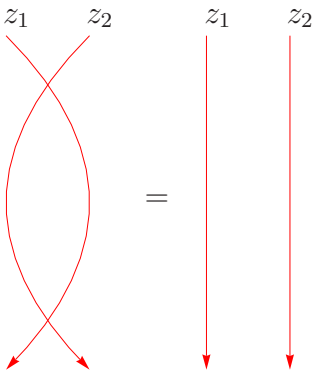


- the crossing relation:

$$R(z,w) = -\left(\frac{w}{z}\right)^2 R^{rot}(-w,z) \tag{26}$$

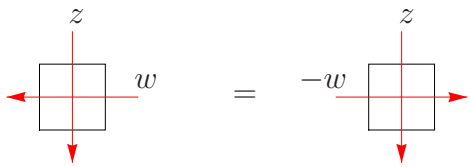


- the Yang-Baxter equation:

$$R_{23}(u,v)R_{12}(u,w)R_{23}(v,w) = R_{12}(v,w)R_{23}(u,w)R_{12}(u,v) \tag{27}$$

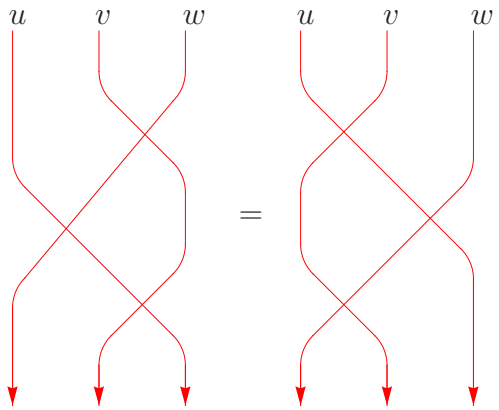


The $K$-matrix satisfies the next equations:

- the boundary inversion/unitarity relation:
  - left boundary:

$$K_l(w,z_B)K_l(w^{-1},z_B) = W_{K_l}(w,z_B)W_{K_l}(w^{-1},z_B)\cdot \mathrm{id} \tag{28}$$

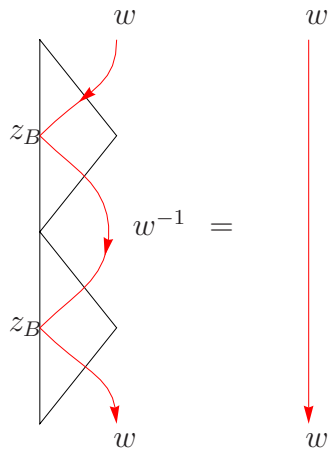


– right boundary:

$$K_r(w, z_B)K_r(w^{-1}, z_B) = W_{K_r}(w, z_B)W_{K_r}(w^{-1}, z_B) \cdot \mathrm{id} \tag{29}$$

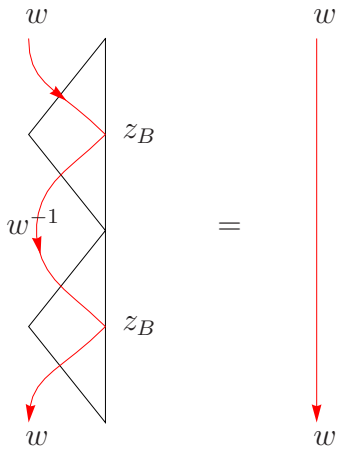


- the boundary crossing relation:

$$K_l(w, z_B) = -K_r(-w^{-1}, -z_B) \tag{30}$$

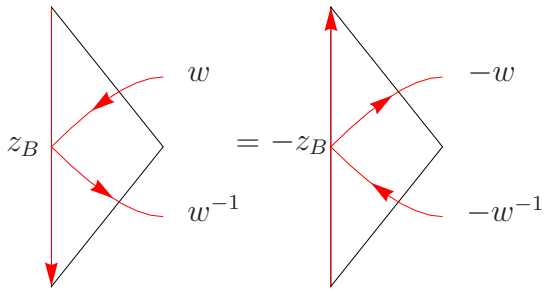


- the reflection equation:

– left boundary:

$$R(v^{-1},u^{-1})K_l(v,z_B)R(u^{-1},v)K_l(u,z_B) = K_l(u,z_B)R(v^{-1},u)K_l(v,z_B)R(u,v) \tag{31}$$

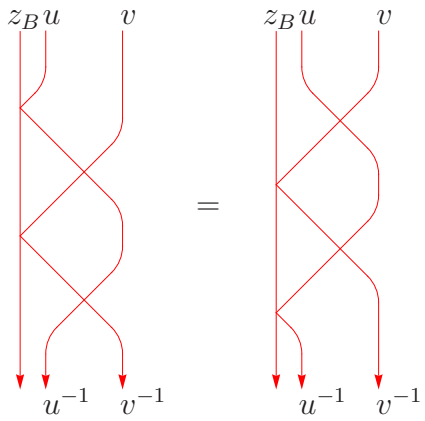


– right boundary:

$$R(v^{-1},u^{-1})K_r(u,z_B)R(u,v^{-1})K_r(v,z_B) = K_r(v,z_B)R(v,u^{-1})K_r(u,z_B)R(u,v) \tag{32}$$

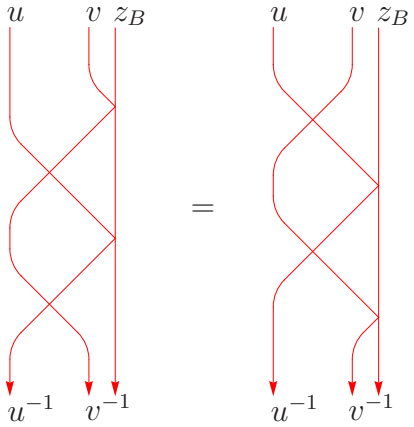


Since there is no restriction on the orientation of the figures, the operators $K_l$ and $K_r$ are related by symmetry, and an inversion of the rapidity line. For our purposes, it is enough to replace $K_r$ with a 'upside-down' left $K_l$-matrix. The next reflection equation holds for this case (The interpretation as operators might seem obscure, however we can always refer to statistical interpretation. Note the direction of rapidities and boundary rapidities):

$$R(u,v^{-1})K_l(u,-z_B)R(v,u^{-1})K_r(v,z_B) = K_r(v,z_B)R(u,v)K_l(u,-z_B)R(v,u^{-1}) \tag{33}$$

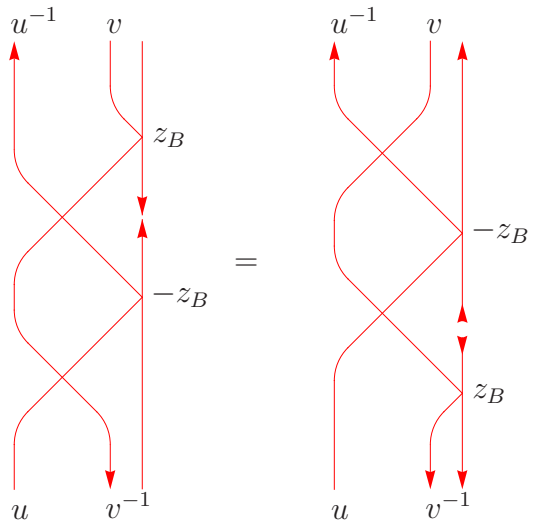


To make the boundary rapidity flows continuous, we introduce the next 'boundary-crossed' left $K$-matrix, by the next definition:

$$K_l^{b.reversed}(w, -z_B) = K_r(w, z_B) \tag{34}$$

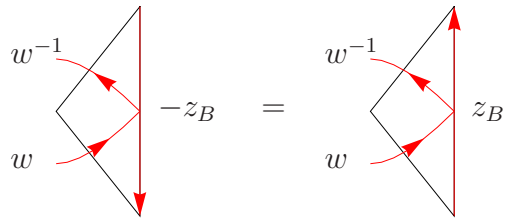


By this, eq. (33) can be written in the next form:

$$R(u, v^{-1})K_l^{b.reversed}(u, z_B)R(v, u^{-1})K_r(v, z_B) = K_r(v, z_B)R(u, v)K_l^{b.reversed}(u, z_B)R(v, u^{-1}) \tag{35}$$

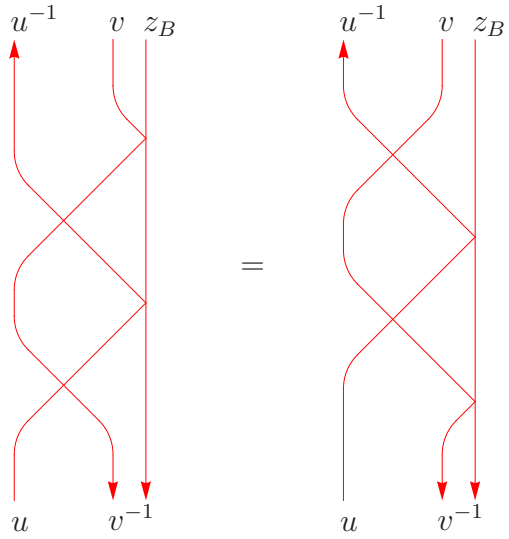

Similarly, we can introduce 'boundary-crossed' right $K$-matrix, however, we do not describe this here, we leave it for the educated reader.

## 2.3 Double row transfer matrix

Based on these definitions, we define the *double row transfer matrix*:

$$T_L(w, \zeta_0, z_1, \ldots, z_L, \zeta_{L+1}) =$$

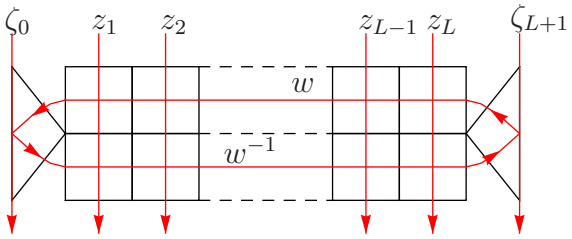


It can be eaily seen , that such double row transfer matrices form a one parameter family of commuting matrices [25]:

$$[T_L(w_i, \zeta_0, z_1, \ldots, z_L, \zeta_{L+1}), T_L(w_j, \zeta_0, z_1, \ldots, z_L, \zeta_{L+1})] = 0 \tag{36}$$

A transfer matrix act on a link pattern as a stochastical operator, sending it to a linear combination of other link patterns, weighted by Laurent polynomials in the rapidities $z_1, \ldots, z_L$ and boundary rapidities $\zeta_0, \zeta_{L+1}$. Note, that the polynomials in the eigenvectors of the transfer matrix do not depend on $w_i$, which is only a spectral parameter, and which we will call *auxiliary rapidity*.

Take a configuration with finite $L$ width and which is infinite upward, with an edge at the bottom. The edge at the bottom is a realization of $dLP_L$. Acting on this configuration with a $T$-matrix is adding the $T$-matrix to the bottom edge, and consider the $dLP_L$ configuration on the new edge. The probability distribution of the link pattern configurations is given by the groundstate eigenvector of the $T$-matrix, which we will denote by $|\Psi(z_0, z_1, \ldots, z_L, z_{L+1})\rangle$, where for simplicity we have changed notation, $\zeta_i \equiv z_i$ for $i = 0, L+1$. The existence and uniqueness of such a vector is provided by the Perron-Frobenius theorem:

$$T\left(w, z_0, \ldots, z_{L+1}\right) |\Psi\left(z_0, \ldots, z_{L+1}\right)\rangle = N\left(w, z_0, \ldots, z_{L+1}\right) |\Psi\left(z_0, \ldots, z_{L+1}\right)\rangle \tag{37}$$

where $N\left(w, z_0, \ldots, z_{L+1}\right)$ is the normalization of the $T$-matrix:

$$N\left(w, z_0, \ldots, z_{L+1}\right) = W_{K_l}(w, z_0) W_{K_l}(w^{-1}, -z_{L+1}) \prod_{i=1}^{L} W_R(w, z_i) W_R(z_i, w^{-1}) +$$
$$\tilde{W}_{K_l}(w, z_0) \tilde{W}_{K_l}(w^{-1}, -z_{L+1}) \prod_{i=1}^{L} \tilde{W}_R(w, z_i) \tilde{W}_R(z_i, w^{-1}) \tag{38}$$

where $W_R$ and $W_{K_l}$ are the normalization of the $R$ and $K_l$-matrices, and $\tilde{W}_R$ and $\tilde{W}_{K_l}$ are the next functions:

$$\tilde{W}_R(z_1, z_2) = W_1(z_1, z_2) - W_t(z_1, z_2) \tag{39}$$

$$\tilde{W}_{K_l}(z, z_B) = K_{id}(z, z_B) + K_m(z, z_B) - K_1(z, z_B) \tag{40}$$

The value of the normalization is non-trivial, since it is not the product of the normalization of the constituting $R$ and $K$-matrices. The derivation for $N$ is in Appendix A. The weight for the $K$-matrix on the right is computed by $K_L^{b.reversed}$.

The groundstate vector is a vector of polynomials in $z_i$, in the basis of $dLP_L$:

$$|\Psi_L(z_0, \ldots, z_{L+1})\rangle = \sum_{\pi \in dLP_L} \psi_\pi(z_0, \ldots, z_{L+1}) \, |\pi\rangle \tag{41}$$

Here $\psi_\pi(z_0, \ldots, z_{L+1})$ is the polynomial coefficient of the basis element $|\pi\rangle$. Sometimes we will use the next notation: $|\psi_\pi\rangle = \psi_\pi(z_0, \ldots, z_{L+1}) \, |\pi\rangle$. It is worth to mention, that even if $z_0$ and $z_{L+1}$ have been introduced differently from the other rapidities, they behave similarly as all the other rapidities. The reason is that an open boundary $K$-matrix can be constructed from a closed boundary $KRR$ configuration, and the vertical rapidity of the $R$-matrices turn into the boundary rapidity. This is explained in details in Appedinx refapp:KmxConstr.

By introducing $dLP_L$, we are able to compute quantities on the half-strip. In order to compute quantities on the full strip, we introduce $dLP_L^*$, the dual space of $dLP_L$. The dual space consist the link patterns in the downward direction, the probabilities of configurations in $dLP_L^*$ are constructed similarly to $dLP_L$. The scalar product of $\langle\psi_\alpha| \in dLP_L^*$ and $|\psi_\beta\rangle \in dLP_L$, $\langle\psi_\alpha|\psi_\beta\rangle$ equals 0, if the two link patterns can not be matched respecting the occupation of the sites, otherwise equals the probability of the full strip configuration.

The transfer-matrix of $dLP_L$ and $dLP_L^*$ are related by the next relation:

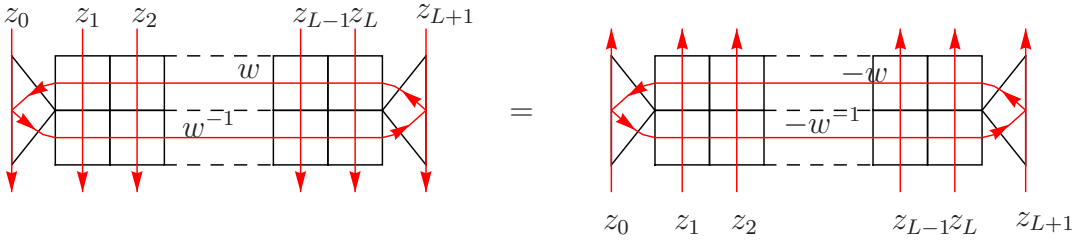


Based on this, the relation between the groundstate elements:

$$\psi_\alpha(z_0, \ldots, z_{L+1}) = \psi_{r(\alpha)}(z_{L+1}, \ldots, z_0) \tag{42}$$

where $\alpha \in dLP_L$ and $r(\alpha) \in dLP_L^*$ are related by a 180 degree rotation, e.g.: $r(|...()(..\rangle) = \langle..)()...|$.

For further calculation, we need to define three quantities: the empty element, the partition sum of the half strip, and the partition sum of the full strip. The $\psi_{EE}$ *empty element* is the link pattern only with unoccupied sites. The *partition sum of the half strip* is the sum of all groundstate elements:

$$Z_{h.s}(z_0,\ldots,z_{L+1}) = \sum_{\alpha\in dLP_L} \psi_\alpha(z_0,\ldots,z_{L+1}) \tag{43}$$

The *partition sum of the full strip* is the normalization of the probabilities on the full strip. The partition sum of the full strip is computable by

$$Z_{f.s.}(z_0,\ldots,z_{L+1}) = \sum_{\alpha,\beta} \psi_\alpha(z_0,\ldots,z_{L+1})\psi_\beta(z_{L+1},\ldots,z_0) \tag{44}$$

where we sum up to $\alpha,\beta \in dLP_L$ link patterns with matching occupation.

Based on the properties of the $R$ and $K$-matrices, the transfer matrix satisfies the interlacing conditions (with suppressing irrelevant notation):

$$R_{i,i+1}(z_i,z_{i+1})T\left(\ldots,z_i,z_{i+1},\ldots\right) = T\left(\ldots,z_{i+1},z_i,\ldots\right) R_{i,i+1}(z_i,z_{i+1}) \tag{45}$$

$$K_l\left(z_1,z_0\right) T\left(z_1,\ldots\right) = T\left(z_1^{-1},\ldots\right) K_l\left(z_1,z_0\right) \tag{46}$$

$$K_r\left(z_L,z_{L+1}\right) T\left(\ldots,z_L\right) = T\left(\ldots,z_L^{-1}\right) K_r\left(z_L,z_{L+1}\right). \tag{47}$$

Acting with both sides on $|\Psi_L\rangle$, we can derive the $q$-Knizhnik-Zamolodchikov equations [3] for the dilute $O(1)$ model, with open boundaries:

$$R_{i,i+1}(z_i,z_{i+1})\left|\Psi\left(\ldots,z_i,z_{i+1},\ldots\right)\right\rangle = W_R(z_i,z_{i+1})\left|\Psi\left(\ldots,z_{i+1},z_i,\ldots\right)\right\rangle \tag{48}$$

$$K_l\left(z_1,z_0\right)\left|\Psi\left(z_1,\ldots\right)\right\rangle = W_{K_l}\left(z_1,z_0\right)\left|\Psi\left(z_1^{-1},\ldots\right)\right\rangle \tag{49}$$

$$K_r\left(z_L,z_{L+1}\right)\left|\Psi\left(\ldots,z_L\right)\right\rangle = W_{K_r}\left(z_L,z_{L+1}\right)\left|\Psi\left(\ldots,z_L^{-1}\right)\right\rangle. \tag{50}$$

# 3 Definition of current, main results

## 3.1 Boundary to boundary current

In this section, we give our main result, the exact finite size expression for the boundary to boundary current in the dilute $O(1)$ model.

The spin-1 currennt, introduced in eq. (1) is equal with with the signed sum of all the possible plaquette configurations, which have boundary to boundary line between the selected vertices. After Baxterization, $F^{(x_1,x_2)}$ and $P(C)$ become a function of the rapidities. Because of the additivity of $F$, it is sufficient to concentrate on two cases, when the two

points are on two adjacent sites. The markers can be separated by a horizontal lattice edge (Using horizontal and vertical lattice-indices for the coordinates $x_1$, $x_2$.):

$$X^{(k)} = F^{((i,k),(i,k+1))}, \tag{51}$$

or a vertical one:

$$Y^{(k)} = F^{((k,j),(k-1,j))} \tag{52}$$

After Baxterization, $X$ and $Y$ become functions of the rapidities and boundary rapidities. Since the commutativity of $T$-matrices (Eq. 36) $X$ depends only on the vertical rapidities, and $Y$ has an extra dependence on the auxiliary rapidity between $k$ and $k-1$:

$$X^{(k)} = X^{(k)}(z_0, \ldots, z_{L+1}), \tag{53}$$

$$Y^{(k)} = Y^{(k)}(w, z_0, \ldots, z_{L+1}). \tag{54}$$

## 3.2 Main result

Our main result is an explicit expression for both $X$ and $Y$ on an inhomogeneous dilute $O(1)$ model, defined on a strip, infinite in both vertical directions, with a finite width $L$. In order to present these expressions, first we introduce some auxiliary functions. We will use the next definition of the elementary symmetric functions:

$$e_k(z_1, \ldots, z_n) = \sum_{1 \le i_1 < \ldots < i_k \le n} z_{i_1} \ldots z_{i_n} \text{ for } 1 \le k \le n, \text{ otherwise } 0 \tag{55}$$

and we introduce elementary symmetric functions over $z_i$'s and $z_i^{-1}$'s:

$$E_i(z_0, z_1, \ldots, z_L, z_{L+1}) = e_i\left(z_0, z_1, \ldots, z_L, z_{L+1}, z_0^{-1}, z_1^{-1}, \ldots, z_L^{-1}, z_{L+1}^{-1}\right) \tag{56}$$

Define two auxiliary functions:

$$V_L(z_0, z_1, \ldots, z_L, z_{L+1}) = \det_{1 \le i,j \le L+1} E_{3j-2i}(z_i) - E_{3j-2i+4(L+2)}(z_i) \tag{57}$$

$$W_L(z_0, z_1, \ldots, z_L, z_{L+1}) = \det_{L+2 \le i,j \le 2L+3} E_{3j-2i}(z_i) + E_{3j-2i+4(L+2)}(z_i) \tag{58}$$

By these definitions, the empty element and the partition sum can be defined [22, 23]:

$$\psi_{L,EE}(z_0, \ldots, z_{L+1}) = \frac{V_L(z_0, \ldots, z_{L+1}) W_L(z_0, \ldots, z_{L+1})}{V_{L+2}(q^2, q, z_0, \ldots, z_{L+1})} \tag{59}$$

$$Z_{L,h.s.}(z_0, \ldots, z_{L+1}) = 2^L \psi_{L,EE}(z_0, \ldots, z_{L+1}) \tag{60}$$

$$Z_{L,f.s.}(z_0, \ldots, z_{L+1}) = 2^L \left(\psi_{L,EE}(z_0, \ldots, z_{L+1})\right)^2 \tag{61}$$

In this paper, we will prove that, on an inhomogeneous lattice of width $L$:

$$X_L^{(i)}(z_0,\dots,z_{L+1}) = \frac{(1-2q)}{2}\frac{z_i^2-1}{z_i E_1(z_0,\dots,z_{L+1})} \tag{62}$$

$$Y_L^{(i)}(w,z_0,\dots,z_{L+1}) = 3(-1)^{L+1}(w-1)^2(w+1)^2 \frac{\psi_{L+2,EE}(w,-w,z_0,\dots,z_{L+1})}{\psi_{L,EE}(z_0,\dots,z_{L+1})E_1(z_0,\dots,z_{L+1})}\frac{w^{2(L+1)}}{W_Y(w,z_0,\dots,z_{L+1})} \tag{63}$$

Here $W_Y(w,z_0,\dots,z_{L+1})$ is an auxiliary function, proportional to the weight of the $T$-matrix:

$$W_Y(w,z_0,\dots,z_{L+1}) = \prod_{i=0}^{L+1} W_R(z_i,w)W_R(w^{-1},z_i) + \prod_{i=0}^{L+1}\tilde{W}_R(z_i,w)\tilde{W}_R(w^{-1},z_i) \tag{64}$$

Notice, that $W_Y$ contains terms which are formally belong to $R$-matrix with the boundary rapidities. $X$ can be written in the next form:

$$X_L^{(i)}(z_0,\dots,z_{L+1}) = \frac{1-2q}{2} z_i \frac{\partial}{\partial z_i}\log E_1(z_0,\dots,z_{L+1}) \tag{65}$$

# 4 Recursion relations

In this section, we derive recursion equations, relating systems with size $L$ and $L-1$. Setting two adjacent rapidities to a special ratio, the system size $L$ effectively decreases by one. The special ratio prohibit certain configurations on the two sites, which results by an effective decrease in the system size. The same mechanism works on the boundary, by setting the boundary rapidity and the first (last) rapidity to the special ratio. This allows us to relate systems of different sizes $L$ and $L-1$ to each other by the recursion relations.
The polynomial weights of the configurations become 0, if the configuration is not allowed, and factorize into a product of a symmetric prefactor and the polynomial weight of the smaller configuration, if it is allowed.
This situation is well known in IQFT literature, usually referred as fusion equation and boundary fusion equation [27].

## 4.1 Fusion equation

The $R$-matrix factorizes into the product of two 'triangle operators', if we set the two variables to $zq^{-1}$, $zq$:

$$R\left(zq^{-1}, zq\right) = (-1-q)M \cdot S =$$
$$(-1-q)\left(\bigtriangledown + \bigtriangledown + \bigtriangledown + \bigtriangledown\right) \cdot \left(\bigtriangleup + \bigtriangleup + \bigtriangleup + \bigtriangleup\right) \quad (66)$$

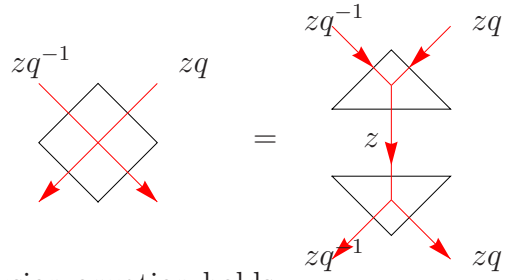


With the help of $M$, the fusion equation holds:

$$R_i(zq, w)R_{i+1}(zq^{-1}, w)M_i = 2\frac{(w-z)(w+z)}{z^2}M_iR_i(z, w) \quad (67)$$

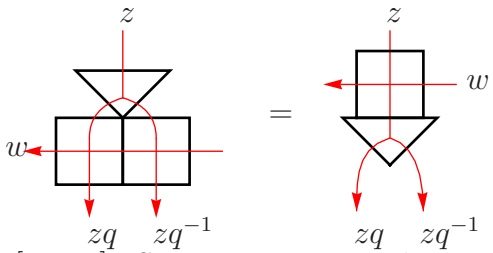


The proof can be found in [22, 23]. Setting $z_i = zq$ and $z_{i+1} = zq^{-1}$ means that we can use the fusion equation from row to row, effectively decrease the system size by one. In fact, the 'triangle operators' are intertwiners between $dLP_L$ and $dLP_{L-1}$. This relates the transfer-matrices:

$$M_iT_L(\ldots, z_i = zq, z_{i+1} = zq^{-1}, \ldots) = T_{L-1}(\ldots, z, \ldots)M_i \quad (68)$$

Act by both sides on $|\Psi_L(\ldots, z_i = zq, z_{i+1} = zq^{-1}, \ldots)\rangle$ and using that $|\Psi\rangle$ is the eigenvector of $T$:

$$M_i\left|\Psi_L(\ldots, z_i = zq, z_{i+1} = zq^{-1}, \ldots)\right\rangle =$$
$$= T_{L-1}(\ldots, z, \ldots)\left(M_i\left|\Psi_L(\ldots, z_i = zq, z_{i+1} = zq^{-1}, \ldots)\right\rangle\right) \quad (69)$$

which using the uniqueness of the eigenvector:

$$M_i\left|\Psi_L(\ldots, z_i = zq, z_{i+1} = zq^{-1}, \ldots)\right\rangle =$$
$$= F(z, z_0, \ldots, z_{i-1}, z_{i+2}, \ldots, z_{L+1})\left|\Psi_{L-1}(\ldots, z, \ldots)\right\rangle \quad (70)$$

where $F(z, z_0, \ldots, z_{i-1}, z_{i+2}, \ldots, z_{L+1})$ is a proportionality factor:

$$F(z; z_1, \ldots, z_n) = \prod_{j=1}^{n} E_1(z, z_j). \tag{71}$$

How $M_i$ maps from $dLP_L$ to $dLP_{L-1}$ depends on the link pattern on the two sites (Here | stands for ( or ) without specification.):

- Mapping to empty site:

$$\begin{aligned} M: \quad & () \to . \\ & .. \to . \end{aligned}$$

- Mapping to one occupied, one empty site:

$$\begin{aligned} M: \quad & .| \to | \\ & |. \to | \end{aligned}$$

- Disappearing elements:

$$M: \quad || \to 0$$

The reason for the recursion relation is clear, if we look at the next qKZ equation:

$$R\left(zq^{-1}, zq\right) \left|\Psi_L\left(\ldots zq^{-1}, zq \ldots\right)\right\rangle = \left|\Psi_L\left(\ldots zq, zq^{-1} \ldots\right)\right\rangle \tag{72}$$

Since $W_2\left(zq^{-1}, zq\right) = 0$, it is impossible to have two not connected line at these sites, effectively decreasing the size by one.

## 4.2 Boundary recursion relations

Based on a very similar argument, as before, we have a recursion relation involving the $K$-matrix. Setting $z_0 = zq$, $z_1 = zq^{-1}$, or $z_L = zq$, $z_{L+1} = zq^{-1}$ is effectively decreases the size of the system by one. The reasoning is basically identical for the left and right boundary, so here we present only the one for the left side.
Setting $z_0 = zq$, $z_1 = zq^{-1}$, the left $K$-matrix factorizes into un upper and a lower triangle:

$$K_l\left(z_1 = zq^{-1}, z_0 = zq\right) = -\frac{-1 + 2q + z^2 + qz^2}{-1 + q + z^2} L_l \cdot U_l =$$

$$-\frac{-1 + 2q + z^2 + qz^2}{-1 + q + z^2} \left( \quad + \quad \right) \cdot \left( \quad + \quad \right) \tag{73}$$

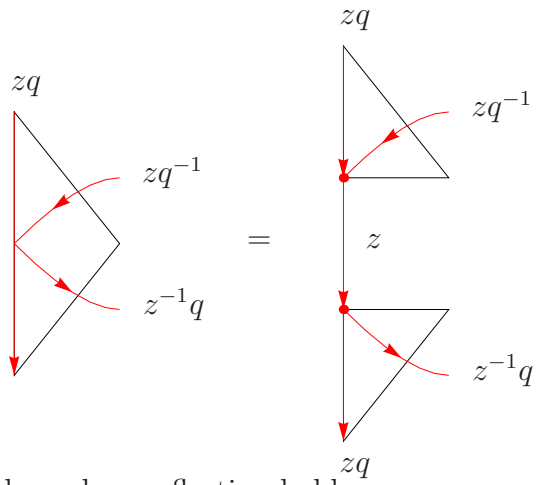


Using the operator $U$, the boundary reflection holds:

$$U_l R_1\left(w^{-1}, zq^{-1}\right) K_l(w, zq) R_1\left(zq^{-1}, w\right) = \\ = \frac{q(w+z)(-1+wz)w^2(1+z^2)^2}{z^2(-w1+qw-qz+qw^2z-qz^2)} K_l(w,z) U_l \quad (74)$$

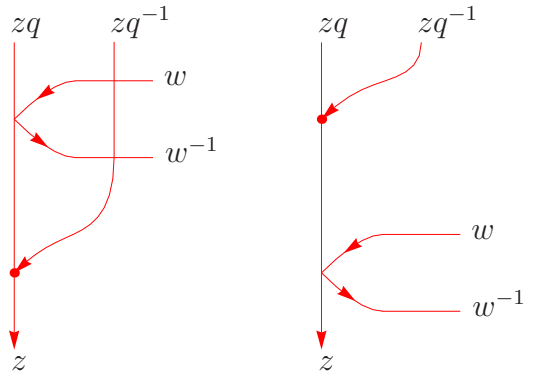


This can be proved by combining the fusion equation and the open boundary $K$-matrix construction described in Appendix B.By this, the next interlacing equation holds:

$$L_l T_L(w, z_0 = zq, z_1 = zq^{-1}, \ldots) = T_{L-1}(w, \ldots, z, \ldots) L_l \quad (75)$$

Similarly, as before, $L_l$ effectively decrease the system size by one:

$$L_l \left|\Psi_L(z_0 = zq, z_1 = zq^{-1}, \ldots)\right\rangle = F(z, z_2, \ldots, z_{L+1}) \left|\Psi_{L-1}(z, z_2 \ldots)\right\rangle \quad (76)$$

where $F(z, z_0, \ldots, z_{i-1}, z_{i+2}, \ldots, z_{L+1})$ is the same proportionality factor (eq. (71)). This recursion relation decrease the system size by effectively erasing the first site. An identical derivation true for the right side, which means, that based on the fusion and the boundary fusion equations, from the recursion point of view, we can treat all the

rapidities and boundary rapidities on the same footing, and in the following, we do not have to distinguish them.

Based on these results, the next recursion relations can be derived for the partition sums:

$$Z_{L,h.s.}\left(\dots z_i = zq, z_{i+1}q^{-1}\dots\right) = 2\sum_{k\neq i,i+1} E_1(z,z_k) Z_{L-1,h.s}\left(\dots z\dots\right) \tag{77}$$

$$Z_{L,f.s.}\left(\dots z_i = zq, z_{i+1}q^{-1}\dots\right) = 2\sum_{k\neq i,i+1} E_1^2(z,z_k) Z_{L-1,f.s}\left(\dots z\dots\right). \tag{78}$$

The factor 2 is coming from the fact, that every smaller GS element has two possible source in the larger system. The $F^2$ proportionality factor in $Z_{L,f.s.}$ is coming from the fact, that it is a sum of products of GS elements.

# 5 Symmetries

## 5.1 Symmetries of $Y_L$

In this section, we will show, that under the assumption, that $Y_L^{(k)}(w; z_0, \dots, z_{L+1})$ is symmetric under $z_i \to z_i^{-1}$, $Y_L^{(k)}$ is independent of the position $k$, and symmetric in the variables $z_0, \dots, z_{L+1}$.

Define $p$ as a path going from the left boundary to the right boundary. The path is defined as a set of $K$ and $R$-matrices, which constitute the line connecting the two boundaries. Regard two paths to be different, if the line connecting the two boundaries are the same, but there is difference between the content of the $K$ and $R$-matrices (E.g. in Fig. 7). By this definition, we identify configurations, which only differ in their position, and which are related by a vertical translation.

The weight of the $p$ path is the weight of the constituting matrices. Since $Y_L^{(k)}$ depends only on one auxiliary rapidity, we set all the auxiliary rapidities to the same value $w$. Denote the weight of $p$ by $\Omega_p(w, z_0 \dots z_{L+1})$.

The set of all paths, $P$ is a union of two disjoint sets, $P_T$ and $P_B$. $P_T$ contains the paths starting from the top of the left $K$-matrix, $P_B$ contains the ones starting from the bottom of it. Every path, $p \in P_T$ is in bijection with a path $\tilde{p} \in P_B$, by a horizontal mirroring (as in Fig. 8). By the properties of the $R$ and $K$-matrices, it is easy to see, that $\Omega_p(w, z_0 \dots z_{L+1}) = \Omega_{\tilde{p}}(w, z_0^{-1} \dots z_{L+1}^{-1})$.

Introduce $m_{p,k,x}$, where $p$ denotes the path, $0 \leq k \leq L+2$ the horizontal position of $Y_L^{(k)}$, and $x \in T, B$ is stands for 'top' or 'bottom'. Define $m_{p,k,x}$ as the signed crossing of the path $p$ at horizontal line $k$ on the 'top' or 'bottom' section, i.e. at the top or bottom of the double row transfer-matrix (See in Fig. 9). Signed crossing means that if the line

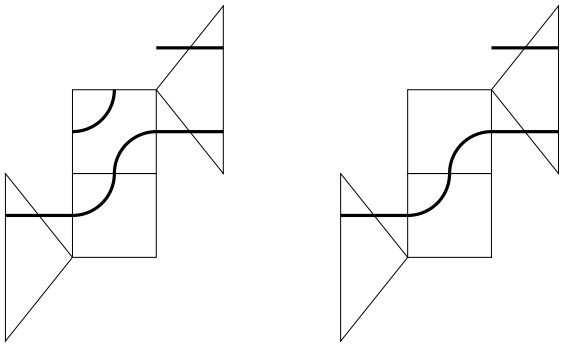

Figure 7: These two paths are not equivalent.

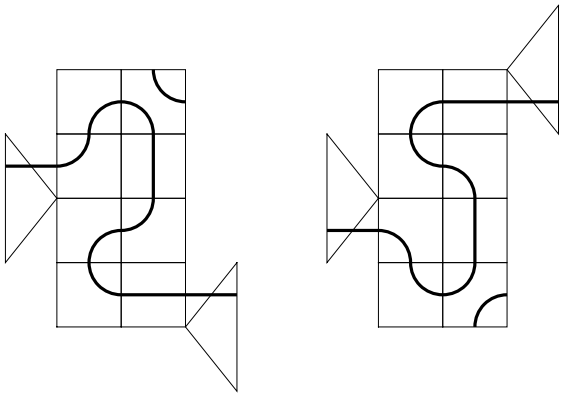

Figure 8: Path $p$ and the mirrored path $\tilde{p}$.

crosses from left to right, it counts as 1, if from right to left, it counts as $-1$. Since a path is crossing once more from left to right then to right to left, $m_{p,k,T} + m_{p,k,B} = 1$ (E.g. in Fig. 9).

By the mirroring, the crossing from the top of the path $p$ maps to the crossing to the bottom of the path $\tilde{p}$, and vice versa. This means, that $m_{p,k,x} = m_{\tilde{p},k,\bar{x}}$, where $\bar{T} = B$, $\bar{B} = T$. Combining these features, it is clear, that $m_{p,k,x} + m_{\tilde{p},k,x} = 1$. Denote by $Y_L^{(k,T)}$ and $Y_L^{(k,B)}$ the current through the top and the bottom of the $T$-matrix, respectively. By this definitions, the $Y$ current is given by:

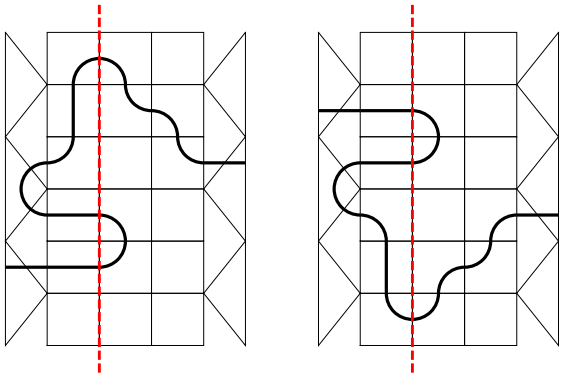

Figure 9: $m_{k=1,p,T} = 2$, $m_{k=1,p,B} = -1$, $m_{k=1,\tilde{p},T} = -1$, $m_{k=1,\tilde{p},B} = 2$

$$Y_L^{(k,x)}(w, z_0, \dots z_{L+1}) = \sum_{p \in P_T} m_{p,k,x} \Omega_p \left(w, z_0, \dots z_{L+1}\right) + \sum_{\tilde{p} \in P_B} m_{\tilde{p},k,x} \Omega_{\tilde{p}} \left(w, z_0, \dots z_{L+1}\right)$$
$$= \sum_{p \in P_T} m_{p,k,x} \Omega_p \left(w, z_0, \dots z_{L+1}\right) + m_{\tilde{p},k,x} \Omega_p \left(w, z_0^{-1}, \dots z_{L+1}^{-1}\right) \quad (79)$$

If we assume, that $Y$ is symmetric under $z_i \to z_i^{-1}$, then we can consider the next construction:

$$Y_L^{(k,x)}(w, z_0, \dots z_{L+1}) = \frac{1}{2}\left(Y_L^{(k,x)}\left(w, \{z_i\}\right) + Y_L^{(k,x)}\left(w, \left\{z_i^{-1}\right\}\right)\right) =$$
$$= \frac{1}{2}\left(\sum_{p \in P_T} m_{p,k,x} \Omega_p \left(w, \{z_i\}\right) + m_{\tilde{p},k,x} \Omega_p \left(w, \left\{z_i^{-1}\right\}\right) + \right.$$
$$\left. + \sum_{p \in P_T} m_{p,k,x} \Omega_p \left(w, \left\{z_i^{-1}\right\}\right) + m_{\tilde{p},k,x} \Omega_p \left(w, \{z_i\}\right)\right) =$$
$$\frac{1}{2}\left(\sum_{p \in P_T} (m_{p,k,x} + m_{\tilde{p},k,x}) \Omega_p \left(w, \{z_i\}\right) + + \sum_{p \in P_T} (m_{p,k,x} + m_{\tilde{p},k,x}) \Omega_p \left(w, \left\{z_i^{-1}\right\}\right)\right) =$$
$$\frac{1}{2} \sum_{p \in P_T} \Omega_p \left(w, \{z_i\}\right) + \Omega_p \left(w, \left\{z_i^{-1}\right\}\right) \quad (80)$$

It thus follows that each path in $P_T$ contribute to $Y$, by the average of the weight of $p$ and $\tilde{p}$. It is also clear from this reasoning, that $Y^{(k)}$ is independent of $k$. This means, there is no further restriction on its symmetries, so it is symmetric in $z_i$, and under $z_i \to z_i^{-1}$, $\forall i$.

### 5.2 Symmetries of $X_L$

It is easy to see, that $X_L^{(i)}$ symmetric in $\{z_0, \ldots, z_{i-1}\}$ and $\{z_{i+1}, \ldots, z_{L+1}\}$, based on the commutativity of $X^{(i)}$ and $R_{j,j+1}$, if $i \neq j, j+1$. For the boundary rapidities $z_0$ and $z_L$, this is clear from the closed boundary construction, i.e. insted of an $L$ size Open boundary system, we regard it as an $L+2$ size closed boundary system, where we indeed can exchange $z_0$, $z_1$ and $z_L$ and $z_{L+1}$ by an $R$-matrix. This construction is describen in Appendix B. An additional symmetry of $X_L^{(i)}$ is the symmetry under $z_j \to z_j^{-1} \, \forall j \neq i$.

Using the additivity property around an elementary plaquette,

$$X^{(i)(\text{mid})} - Y^{(i+1)} - X^{(i)(\text{top})} + Y^{(i)} = 0. \tag{81}$$

Since $Y$ is position independent, this implies, that $X$ in the middle of the $T$-matrix has the same properties, as the one on the edge.

## 6 Proof of the main result

The $X$ and $Y$ current satisfies the next recursion relations

$$X_L^{(i)}(z_j = zq, z_{j+1} = zq^{-1}) = X_{L-1}^{(i)}(z) \quad \forall i \neq j, j+1 \tag{82}$$

$$Y_L(z_j = zq, z_{j+1} = zq^{-1}) = Y_{L-1}(z) \quad \forall i \neq j, j+1. \tag{83}$$

Note, that depending if $j$ smaller or larger then $i$, the actual position of the current might change, however, we will misuse $X^{(i)}$ to denote both cases. Because of the symmetry properties of $X$ and $Y$, the recursion relations can be extended to not-adjecent rapidities. Our strategy in both case is the follows: First we list the recursion relation for the *unnormalized* expressions $X_{u.n.}$ and $Y_{u.n.}$, and based on that, we prove the recursion relation for the normalized ones.

### 6.1 Proof for the $Y$ current

In Section (5.1) we have seen, that $Y_L(w, z_0, \ldots, z_{L+1})$ symmetric in all the $z_i$'s, and under $z_i \to z_i^{-1}$. The unnormalized version of $Y$ is computable in the next way:

$$Y_L^{(i),u.n.} = \sum_{\alpha,\beta,\gamma} (-1)^{sign(\alpha,\beta,\gamma)} \psi_\alpha T_\beta \psi_\gamma. \tag{84}$$

Here, $\psi_\alpha \in dLP_L$, $\psi_\gamma \in dLP_L^*$ and $T_\beta$ is a T-matrix configuration, which provides the necessary tiles, to have a path through the top row of the $T$-matrix, at position $i$, $sign(\alpha, \beta, \gamma) = \pm 1$ according to the direction. The relation between the normalized and unnormalized $Y$ current is

$$Y_L^{(i)} = \frac{Y_L^{(i),u.n.}}{Z_{L,f.s.} W_{T,L}}. \tag{85}$$

Here $W_{T,L}$ is the normalization of the $T$-matrix.
Since the recursion relation is known for $Y_L^{(i)}$ (eq. 83) and $Z_{L,f.s}$ (eq. 78):

$$\left.\frac{Y_L^{(i),u.n.}}{W_{T,L}}\right|_{z_j=zq, z_{j+1}=zq^{-1}} = 2\left(\prod_{k\neq j,j+1} E_1^2(z,z_k)\right)\frac{Y_{L-1}^{(i),u.n.}}{W_{T,L-1}} \tag{86}$$

Since $Y$ is fully symmetric (Section (5.1)), and $W_T$ is not fully symmetric, $Y^{u.n.}$ is not symmetric. To exploit the symmetric properties, we introduce auxiliary Laurent-polynomial function, which is symmetric by construction:

$$\tilde{Y}_L^{u.n.} = Y_L^{u.n.}\frac{W_{Y,L}}{W_{T,L}} \tag{87}$$

$W_Y$ is a predefined quantity with the next recursion relation (which can be checked by simple calculation):

$$W_{Y,L}(z_i = zq, z_{i+1} = zq^{-1}) = -w^2 E_1(w,z)E_1(-w1,z)W_{Y,L-1}(z) \tag{88}$$

Now, we can write up the recursion relation for $\tilde{Y}^{u.n.}$, based on the previous equations:

$$\tilde{Y}^{u.n.}(z_i = zq, z_j = z(q)^{-1}) = -2w^2 E_1(w,z1)E_1(-w,z1)\prod_{k\neq i,j} E_1^2(z,z_k)\tilde{Y}^{u.n.}(z) \tag{89}$$

Since $Y$ is fully symmetric, the two rapidities set to given ratio is not restricted to adjacent rapidities. Because of the symmetry under $z_i \to z_i^{-1}$, the recursion relation holds for two additional values. The full set of recursion relations involving two chosen variables $z_i$, $z_j$:

$$Y_L(z_i = zq, z_j = zq^{-1}) = Y_{L-1}(z) \tag{90}$$
$$Y_L(z_i = zq^{-1}, z_j = zq) = Y_{L-1}(z) \tag{91}$$
$$Y_L(z_i = (zq)^{-1}, z_j = z^{-1}q) = Y_{L-1}(z) \tag{92}$$
$$Y_L(z_i = z^{-1}q, z_j = (zq)^{-1}) = Y_{L-1}(z) \tag{93}$$

Since involving two chosen variables, there are 4 recursion relations, with one chosen variable $z_k$, there are $4(L+1)$ recursion relations relating $Y_L$ and $Y_{L-1}$, fully exploiting symmetry and inversion symmetry.

$\tilde{Y}^{u.n.}$ has been calculated for $L = 0, 1, 2$, giving starting element for the next form:

$$\begin{aligned}&\tilde{Y}^{u.n.}(w, z_0, \ldots, z_{L+1}) = \\ &= 2^L 3(-1)^{L+1} w^{2(L+1)}(w-1)^2(w+1)^2 \frac{\psi_{L,EE}(z_0\ldots,z_{L+1})\psi_{L+2,EE}(w,-w,z_0\ldots,z_{L+1})}{E_1(z_0,\ldots,z_{L+1})}\end{aligned} \tag{94}$$

The degree width of this expression is $4(L+1)-1$ for system size $L$, which means that the recursion fully fixes $\tilde{Y}^{u.n.}$ for any system size, as a Lagrange interpolation. From this, based on eq. (87), we have $Y$ for any system size. Since $Y_L = \frac{\tilde{Y}_L^{u.n.}}{Z_{L,f.s.}W_{Y,L}}$, the $Y$ current has the proposed form of eq. (63):

$$Y_L^{(i)}(w, z_0, \ldots, z_{L+1}) = 3(-1)^{L+1}(w-1)^2(w+1)^2 \\ \frac{\psi_{L+2,EE}(w, -w, z_0, \ldots, z_{L+1})}{\psi_{L,EE}(z_0, \ldots, z_{L+1})E_1(z_0, \ldots, z_{L+1})} \frac{w^{2(L+1)}}{W_Y(w, z_0, \ldots, z_{L+1})}$$

By this, based on the recursion relation, we proved that, the unique solution, which satisfies eq. (83) with the computed starting element, is indeed eq. (63).

## 6.2 Proof for the $X$ current

As an unnormalized quantity, we can compute $X$ in the next way:

$$X_L^{(i)u.n.} = \sum_{\alpha,\beta}(-1)^{sign(\alpha,\beta)}\psi_\alpha\psi_\beta \tag{95}$$

where $\psi_\alpha \in dLP_L$, $\psi_\beta \in dLP_L^*$, $\alpha$ and $\beta$ are chosen such, that they form a boundary to boundary line through the site $i$, and $sign(\alpha,\beta) = \pm 1$ according to the direction. The relation between the normalized and unnormalized $X$ current:

$$X_L^{(i)} = \frac{X_L^{(i)u.n.}}{Z_{L,f.s.}} \tag{96}$$

Since $Z_{L,f.s.}$ is fully symmetric, $X_L^{(i)}$ and $X^{(i)u.n.}$ share the same symmetry properties. The recursion relation for $X^{(i)u.n.}$:

$$X_L^{(i)u.n.}(z_j = zq, z_k = zq^{-1}) = 2\prod_{n\neq j,k} E_1^2(z, z_n)X_{L-1}^{(i)u.n.}(z) \tag{97}$$

This quantity has been computed explicitly for $L = 1, 2, 3$, and give hint for the next conjectured form:

$$X_L^{(i)u.n.}(z_0, \ldots, z_{L+1}) = (2-q)2^{L-1}\frac{z_i^2-1}{z_i}\frac{\psi_{L,EE}(z_0, \ldots, z_{L+1})}{E_1(z_0, \ldots, z_L)} \tag{98}$$

Based on the recursion properties of $\psi_L$ and $E_1$, this form clearly satisfies eq. (82). To prove the uniqueness of the solution, we will assume the symmetry in all the variables expect $z_i$. The degree width of $X^{(i)u.n.}$ in any $z_j \neq z_i$ rapidity is $4L-1$. Based on a similar counting as in the $Y$, there are $4L$ recursion relations relating systems $L$ and

$L-1$, since all the arguments hold as for $Y$, only the number of variables is smaller by one (since $X^i$ is not symmetric in $z_i$, but all the other $z$'s.). By this, we see, that under the aforementioned assumption, we have found the unique solution for $X$ described in eq. (62):

$$X_L^{(i)}(z_0,\ldots,z_{L+1}) = \frac{(1-2q)}{2}\frac{z_i^2-1}{z_i E_1(z_0,\ldots,z_{L+1})}$$

# 7 Acknowledgment

GF is grateful to Alexandr Garbali, Kayed Al-Qasimi, Jesper Stokman, Jan de Gier and Paul Zinn-Justin for useful discussion.

# A Normalization of the transfer-matrix

In order to prove the form of the normalization, first, we map the dilute $O(1)$ loop model to a site percolation model, and compute the normalization in the percolation model, using the all-1 left eigenvector.
There is a mapping between the dilute $O(1)$ loop model, and the site percolation model. The site percolation model is built up from randomly distributed spins taking the values $s=\pm 1$ on the vertices of the tiles. The mapping takes place, as the lines of the loop model are mapped to the domain walls of the site percolation. To implement the $R$ and $K$-matrix weight, we introduce the next plaquette-interactions:

- For the $R$-matrix: $R = a + bs_1s_2s_3s_4$
- For the $K$-matrix: $K = A + Bs_1s_3$

Here $s_1, s_2, s_3, s_4$ are the four spins in the corner of the $R$-matrix, and $s_1, s_3$ are the vertices in the upper and lowermost corner of the $K$-matrix. The aforementioned definitions coincide with the loop weights, if

$$a = \frac{1}{2}\left(W_e + W_{R_1}\right) \equiv \frac{1}{2}W_R \tag{99}$$

$$b = \frac{1}{2}\left(W_e - W_{R_1}\right) := \frac{1}{2}\tilde{W}_R \tag{100}$$

$$A = \frac{1}{2}\left(W_{K_e} + W_{K_{OpCl}}\right) \equiv \frac{1}{2}W_K \tag{101}$$

$$B = \frac{1}{2}\left(W_{K_e} + W_{K_{OpCl}}\right) := \frac{1}{2}\tilde{W}_K. \tag{102}$$

We define a percolation state, as a sequence of spins along the bottom line of the $T$-matrix. A percolation state is equal to the sum of loop states with the same occupations,

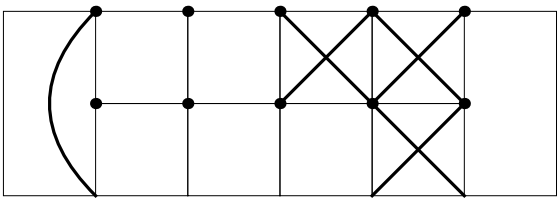

Figure 10: Graphical representation of a summand in the normalization of the percolation transfer-matrix. For better understanding, we denote the $K$-matrices by rectangulars, instead of triangles. The spins –we sum up to– are emphasized by dots.

regardless the connectivity of occupied sites. If we choose to map the occupied sites to $-1$, and the empty ones to $+1$, e.g. $|-1,-1,1,1\rangle_{\text{perco}} = |()..\rangle + |((..\rangle + |))..\rangle + |)(..\rangle$. Even the states are not in bijection, the $T$-matrix configurations are, consequently the normalization for both $T$-matrices are the same.

By definition, the $T$-matrix is a left stochastic matrix, so all the columns of it sum to $N$. Consequently, the left eigenvector is the $(1,1,\ldots,1)$ vector. The corresponding normalization is proportional to the weight of summing over all possible spin configurations of the sites, with the exception of the bottom line, where the resulting states is. The weight of a $T$-matrix is $\prod R \prod K$, and the normalization is

$$N = \frac{\sum_{\text{all config.}} \prod R \prod K}{\sum_{\text{all config.}} 1} = 2^{-2(L+1)} \sum_{\text{all config.}} \prod (a + b s_1 s_2 s_3 s_4) \prod (A + B s_1 s_3). \quad (103)$$

Expanding the products, the summands of $N$ are polynomials in $s_i$, and because $s_i$ is summed over $+1$ and $-1$, if at least one $s_i$ has odd power, the contribution of that summand is 0. It is easy to see, that all the summand has at least one odd-powered $s_i$, with the exception of $\prod a \prod A$ and $\prod b \prod B$. If we represent the $b s_1 s_2 s_3 s_4$ term by a cross at the given square, and $B s_1 s_3$ as a line connecting $s_1$ and $s_3$, a given summand is a partial filling of the $T$-matrix with crosses and lines (Fig. 10), and the power of a spin is equal with the lines starting from that vertex. By putting somewhere a cross or a line, it is clear, that the full $T$-matrix has to be filled in order to not to have vertex with odd lines.

By this, we see, that the only non-vanishing contributions are $\prod a \prod A$ (the "empty" $T$-matrix) and $\prod b \prod B$ (the "completely filled" $T$-matrix). Consequently, the normalization is $N = 2^{-2(L+1)} \sum_{\text{all config.}} \prod a \prod A + \prod b \prod B = \prod a \prod A + \prod b \prod B$. The prefactor coming from the summation cancels the $\frac{1}{2}$ factors, so including inhomogeneous weights:

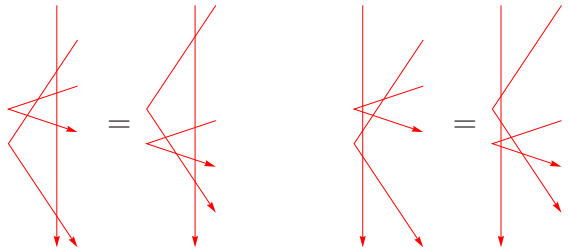

(a) (b)

Figure 11: The construction of a new $K$-matrix via insertion of a line.

$$N\left(w,z_0,\ldots,z_{L+1}\right)=W_{K_l}(w,z_0)W_{K_l}(w^{-1},-z_{L+1})\prod_{i=1}^{L}W_R(w,z_i)W_R(z_i,w^{-1})+$$
$$\tilde{W}_{K_l}(w,z_0)\tilde{W}_{K_l}(w^{-1},-z_{L+1})\prod_{i=1}^{L}\tilde{W}_R(w,z_i)\tilde{W}_R(z_i,w^{-1}) \quad (104)$$

# B Construction of the open boundary $K$-matrix from the closed boundary $K$-matrix via insertion of a line

In this section, we show the construction of the open boundary $K$-matrix weights from the closed boundary case, by the well known method of insertion of a line. The main advantage of this description of the open boundary $K$-matrix, that we can extend the symmetry arguments to the boundary rapidities, and also using the fusion equation, we can deduce the boundary fusion equation immediately.

The closed boundary $K$-matrix consist two elements, with identical weights, and satisfies the reflection equation:

$$K_{\text{closed b.c.}}=$$ 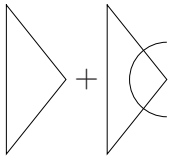 (105)

$$K_{\text{cbc}}R\left(v^{-1},u\right)K_{\text{cbc}}R\left(u,v\right)=R\left(v^{-1},u^{-1}\right)K_{\text{cbc}}R\left(u^{-1},v\right)K_{\text{cbc}} \quad (106)$$

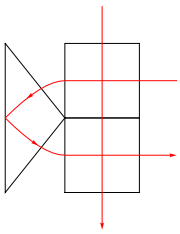

Figure 12: A $KRR$ block. The vertical rapidity is the boundary rapidity of the open B.C. $K$-matrix, the bouncing rapidity is the normal one.

The idea of the insertion of a line is as in Fig. 11 [1]. You multiply the reflection equation from the right with a column of four $R$-matrices, and by the means of the Yang-Baxter equation, you move the $R$-matrices inside (Fig. 11, (b)). In this configuration you can regard the $KRR$ blocks, as the elements of the new $K$-matrix, and the weight of the new $K$-matrix is equal to the sum of the weights of the corresponding $KRR$ blocks (Fig. 12).

Our aim is to follow this procedure to create the open boundary (left) $K$-matrix. (The procedure is the same for the right boundary.) Since we want to create *independent* weights, and the possible $KRR$ configurations depend on if a line or an empty site is entering on the top of the top $R$-matrix, we can elaborate our procedure. For every open boundary $K$-matrix element, we want to have two groups of $KRR$ configurations, one with an entering line on the top, one without, and we expect the sum of these weights to be equal, in order to produce independent open $K$-matrix weights (Figure is needed). Since we expect the right sides of the two $R$-matrix to be the top and bottom half of the open boundary $K$-matrix, the occupancy on the left and on the top already defines the six groups associated with the empty, the top, and the bottom type $K$-matrix. (First three row of the table.)

Distinguishing the two remaining elements (the 'line': and the 'monoid': ) is a bit more tricky, and can be done in the next way: We look at configurations with a line entering, and we group them according to their connectivity on the left: If the two left side are connected, they belong to the 'line', if not, they belong to the 'monoid'. Now we have to choose the other two groups according to the criteria, that with and without the line, the weights should be the same. Based on this criteria, we can uniquely make the choice, however, there is one $KRR$ configuration, which has to 'divided' between the line and the monoid. Regardless these divided cases, the next statement hold for the weight of the open B.C. $K$-matrix and the weight of the $KRR$ configuration:

[1] In this figure –for convenience– we use different style, then in the previous equation. Straight lines represent the rapidity-lines, a crossing of two rapidity lines is an $R$-matrix, a cusp in a line is an $K$-matrix.

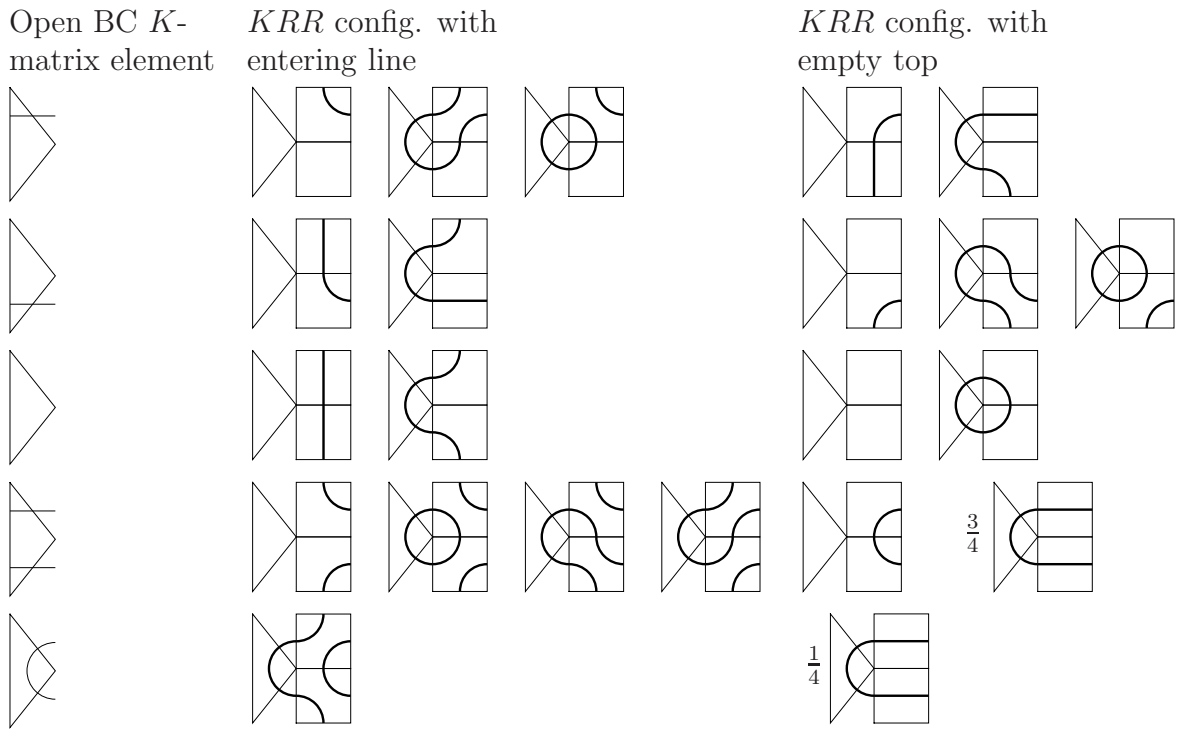


Table 1: Open B.C. $K$-matrix elements expressed by closed B.C. $KRR$ configurations. Note the $\frac{3}{4}$ and $\frac{1}{4}$ factors: In order to reproduce the open B.C. weights, we have to split the configuration into two part, with certain probabilities. These probabilities goes into $\frac{3}{4}$ and $\frac{1}{4}$ in the homogenous limit. For the general expression, consult the text.

$$\frac{\left(1+z_B^2\right)^2 z_1^2}{zB^2} W_{K_{obc}}(z_1, z_B) = \sum_{i \in G_{K_obc}} R_{i,\text{top}}(z_B, z_1) R_{i,\text{bottom}}(z_1^{-1}, z_B) \tag{107}$$

Here $W_{K_{obc}}$ stand for the weigh of a specific open B.C. $K$-matrix element, and the sum on the other side runs over the $KRR$ configurations, which contribute to the given open B.C. $K$-matrix element (As given on Table 1). The divided cases have the prefactors $\frac{3}{4}$ and $\frac{1}{4}$ in the homogeneous case, in the inhomogeneous case, the next relations hold:

$$\begin{aligned}\frac{\left(1+z_B^2\right)^2 z_1^2}{zB^2} W_m^l(z_1, z_B) = W_t(z_B, z_1) W_t\left(z_1^{-1}, z_B\right) + \\ \left(\frac{1}{f\left(z_1^{-1}, z_B\right)+1} + \frac{1}{\left(f\left(z_B, z_1\right)+1\right)\left(f\left(z_B, z_1^{-1}\right)+1\right)}\right) \cdot \\ \cdot W_1(z_B, z_1) W_1\left(z_1^{-1}, z_B\right)\end{aligned} \tag{108}$$

$$\frac{\left(1+z_B^2\right)^2 z_1^2}{zB^2} W_i^l d(z_1, z_B) = \frac{f\left(z_B, z_1^{-1}\right)+1}{f\left(z_1, z_B\right)+1} W_1(z_B, z_1) W_1\left(z_1^{-1}, z_B\right) \tag{109}$$

Where $f$ is defined as:

$$f(z_1, z_2) = \frac{W_2(z_1, z_2)}{W_m(z_1, z_2)}, \tag{110}$$

with the property: $f^{-1}(z_1, z_2) = f(z_2, z_1)$. The prefactors, involving the $f$'s turn into $\frac{3}{4}$ and $\frac{1}{4}$, if the rapidities are equal to 1.
An intuitive understanding of the divination of this $KRR$ configuration is missing, however, the aforementioned relations have been thoroughly checked analytically.
Since the vertical rapidity become the boundary rapidity, the previous argument about the symmetry in the rapidities can be extended to the boundary rapidities too.
It is easy to prove the boundary fusion relation, based on this construction and the fusion relation. If we extend the $KRR$ configuration into a $KRRRR$ configuration, and we apply the recursion relation on the four $R$-matrix, we get the boundary fusion relation, as a corollary.

# References


[1] Bernard Nienhuis. "Critical spin-1 vertex models and $O(n)$ models". *Int. J. Mod. Phys. B 4, 929-942*, 1990.

[2] Bernard Nienhuis. "Critical and multicritical $O(n)$ models". *Physica A 163, 152-157*, 1990.

[3] P. Di Francesco and P. Zinn-Justin. Around the Razumov–Stroganov conjecture: proof of a multi-parameter sum rule. *Electron. J. Combin.*, 12:Research Paper 6, 27 pp, 2005, math-ph/0410061.

[4] Luigi Cantini. qKZ equations and ground state of the O(1) loop model with open boundary conditions. 2009, math-ph/0903.5050.

[5] Jan de Gier, Anita Ponsaing, and Keiichi Shigechi. Exact finite size groundstate of the O(n=1) loop model with open boundaries. *J. Stat. Mech.*, 0904:P04010, 2009, math-ph/0901.2961.

[6] Yacine Ikhlef and Anita Ponsaing. Finite-size left-passage probability in percolation. *J. Stat. Phys. 149 , pp. 10—36.*, 2012, math-ph/1202.5476.

[7] Jan de Gier, Bernard Nienhuis, and Anita Ponsaing. Exact spin quantum hall current between boundaries of a lattice strip. *Nucl. Phys. B 838, 371-390*, 2010, math-ph/1004.4037.

[8] Luigi Cantini. Finite size emptiness formation probability of the XXZ spin chain at $\Delta = -1/2$. 2011, math-ph/1110.2404.

[9] Britta Aufgebauer and Andreas Klümper. Finite temperature correlation functions from discrete functional equations. *J. Phys.*, A: Math. Theor. 45:345203, 2012, cond-mat.stat-mech/1205.5702.

[10] S. Mitra, B. Nienhuis, J. de Gier, and M. T. Batchelor. Exact expressions for correlations in the ground state of the dense O(1) loop model. *J. Stat. Mech.*, 2004(09):P09010, 2004, cond-mat/0401245.

[11] Saibal Mitra and Bernard Nienhuis. Exact conjectured expressions for correlations in the dense O(1) loop model on cylinders. *J. Stat. Mech.*, 2004:P10006, 2004, cond-mat/0407578.

[12] A. V. Razumov and Yu. G. Stroganov. Spin chains and combinatorics. *J.Phys.*, A34:3185, 2001, cond-mat/0012141.

[13] A. V. Razumov and Yu. G. Stroganov. Combinatorial nature of ground state vector of O(1) loop model. *Theor.Math.Phys.*, 138:333–337, 2004, arXiv:math/0104216.

[14] A. V. Razumov and Yu. G. Stroganov. Spin chains and combinatorics: twisted boundary conditions. *J. Phys.*, A: Math. Theor. 34:5335–5340, 2001, math-ph/0102247.

[15] M.T. Batchelor, J. de Gier, and B. Nienhuis. The quantum symmetric XXZ chain at $\Delta = -1/2$, alternating sign matrices and plane partitions. *J.Phys.*, A 34:L265–L270, 2001, cond-mat/0101385.

[16] P. Di Francesco, P. Zinn-Justin, and J.-B. Zuber. Sum rules for the ground states of the O(1) loop model on a cylinder and the XXZ spin chain. *J. Stat. Mech.*, P08011, 2006, math-ph/0603009.

[17] Luigi Cantini and Andrea Sportiello. Proof of the Razumov-Stroganov conjecture. 2010, math.CO/1003.3376.

[18] Murray T. Batchelor. The surprising connection between exactly solved lattice models and discrete holomorphicity. *in Symmetries and Groups in Contemporary Physics (World Scientific Publishing, Singapore)*, pages 31–40, 2013, math-ph/1211.5850.

[19] Jan de Gier, Alexander Lee, and Jorgen Rasmussen. Discrete holomorphicity and integrability in loop models with open boundaries. *J. Stat. Mech., P02029*, 2013, math-ph/1210.5036.

[20] A. G. Izergin and V. E. Korepin. The inverse scattering method approach to the quantum Shabat-Mikhailov model. *Commun. in Math. Phys.*, 79(3):303–316, 1981.

[21] Alexandr Garbali. The domain wall partition function for the Izergin-Korepin 19-vertex model at a root of unity. 2014, math-ph/1411.2903.

[22] Alexandr Garbali and Bernard Nienhuis. "The dilute Temperley-Lieb O($n = 1$) loop model on a semi infinite strip: the ground state". 2014, math-ph/1411.7020.

[23] Alexandr Garbali and Bernard Nienhuis. "The dilute Temperley-Lieb O($n = 1$) loop model on a semi infinite strip: the sum rule". 2014, math-ph/1411.7160.

[24] R. J. Baxter. *"Exacty Solved Models in Statistical Mechanincs"*. Academic Press Ltd., 1982.

[25] E. K. Sklyanin. Boundary conditions for integrable quantum systems. *Journal of Physics A: Mathematical and General*, 21(10):2375, 1988.

[26] Uwe Grimm. Dilute Algebras and Solvable Lattice Models. *Statistical Models, Yang-Baxter Equation and Related Topics, Proceedings of the Satellite Meeting of STATPHYS-19, Tianjin 1995, edited by M.L. Ge and F.Y. Wu, (World Scientific, Singapore)*, pages 110–117, 1996, q-alg/9511020.

[27] Subir Ghoshal and Alexander Zamolodchikov. Boundary S-Matrix and Boundary State in Two-Dimensional Integrable Quantum Field Theory. *Int.J.Mod.Phys.*, A9:3841–3886, 1994, hep-th/9306002.